

## Article

# Electrocatalytic Degradation of Azo Dye by Vanadium-Doped TiO<sub>2</sub> Nanocatalyst

Jih-Hsing Chang <sup>1</sup>, Yong-Li Wang <sup>2</sup>, Cheng-Di Dong <sup>3</sup> and Shan-Yi Shen <sup>1,\*</sup><sup>1</sup> Department of Environmental Engineering and Management, Chaoyang University of Technology, 168 Jifeng E. Rd., Wufeng District, Taichung 41349, Taiwan; changjh@cyut.edu.tw<sup>2</sup> Department of Civil Environmental and Construction Engineering, Texas Tech University, 2500 Broadway, Lubbock, TX 79409, USA; aenguswang8@gmail.com<sup>3</sup> Department of Marine Environmental Engineering, National Kaohsiung University of Science and Technology, 142, Haijhuang Rd., Nanzih District, Kaohsiung 81157, Taiwan; cddong@nkust.edu.tw

\* Correspondence: shanyi0226@gmail.com; Tel.: +886-4-23323000 (ext. 4520); Fax: +886-4-23742365

Received: 6 March 2020; Accepted: 27 April 2020; Published: 28 April 2020



**Abstract:** In this work, nano V/TiO<sub>2</sub> catalysts at different molar ratios were prepared and fabricated as the electrocatalytic electrodes for electrocatalytic degradation. The effect of the vanadium doping on the surface morphology, microstructural, and specific surface area of V/TiO<sub>2</sub> catalysts was probed by field emission scanning electron microscope (FESEM) x-ray diffractometer (XRD), and Brunauer–Emmett–Teller (BET), respectively. Afterward, the solution of Acid Red 27 (AR 27, one kind of azo dye) was treated by an electrocatalytic system in which the nano V/TiO<sub>2</sub> electrode was employed as the anode and graphite as the cathode. Results demonstrate that AR 27 can be effectively degraded by the nano V/TiO<sub>2</sub> electrodes; the highest removal efficiency of color and total organic carbon (TOC) reached 99% and 76%, respectively, under 0.10 VT (molar ratio of vanadium to titanium) condition. The nano V/TiO<sub>2</sub> electrode with high specific surface area facilitated the electrocatalytic degradation. The current density of 25 mA cm<sup>−2</sup> was found to be the optimum operation for this electrocatalytic system whereas the oxygen was increased with the current density. The electricity consumption of pure TiO<sub>2</sub> and nano V/TiO<sub>2</sub> electrode in this electrocatalytic system was around 0.11 kWh L<sup>−1</sup> and 0.02 kWh L<sup>−1</sup>, respectively. This implies that the nano V/TiO<sub>2</sub> electrode possesses both high degradation and energy saving features. Moreover, the nano V/TiO<sub>2</sub> electrode shows its possible repeated utilization.

**Keywords:** dye wastewater; electrocatalyst; titanium dioxide; vanadium-doped

## 1. Introduction

Textile wastewater containing dyes possesses some undesirable qualities such as high color, extreme pH variation, high temperature, high chemical oxygen demand (COD), and low biodegradability. These characteristics make wastewater more complicated, which results in a highly difficult treatment to meet discharge standards [1,2]. The quantity of dyes produced in the world is about 800,000 tons each year, in which half of these are azo dyes. Azo dyes are not only widely used in the textiles industry, but are also used in printing and cosmetics manufacturing [3]. Unfortunately, 15–25% of the dye will be lost during the dying process and maybe directly released into the environment. Once the high color wastewater is accidentally discharged into natural water bodies such as rivers and lakes, the biological self-purification of the water body will be disturbed and cause damage to the ecological environment [4,5].

To effectively remediate such wastewater, advanced oxidation processes (AOPs) have been widely employed. AOP techniques include photocatalysis, Fenton oxidation, electrocatalytic oxidation,

and a combination of the above processes [6–9]. Among these AOPs, the electrocatalytic technique presents several advantages including easy operation, simple instrumentation, and little sludge generation [10,11]. In an electrocatalytic system, the direct current is applied to the catalytic material (usually served as the anode) to produce strong oxidants (i.e.,  $\bullet\text{OH}$ ), which effectively destroys organic contaminants by the oxidation reaction [8]. The electrocatalytic oxidation mainly depends on the process of electron transfer to yield such “clean” oxidants (water molecule spilt) [12]. Based on our previous research, the production rates of  $\bullet\text{OH}$  per unit area and power was  $4.5 \times 10^{-5} \text{ M/W cm}^2$  and  $3.9 \times 10^{-5} \text{ M/W cm}^2$  by the electrocatalytic and photocatalytic systems, respectively [13]. Accordingly, the electrocatalytic oxidation demonstrates better  $\bullet\text{OH}$  production rates under the same applied energy and catalyst surface area. The research also suggests that an electrocatalytic system executes better organic pollutant degradation for wastewater treatment.

The electrode material plays a key role in the electrocatalytic process, and many materials such as  $\text{TiO}_2$ ,  $\text{PbO}_2$ ,  $\text{SnO}_2$ , and boron-doped diamond (BDD) have been investigated for decades. Among the many kinds of electrocatalysts,  $\text{TiO}_2$  is relatively cheap and has the properties of strong oxidation capacity, high chemical stability, and high energy gap [14,15], therefore, it has been widely used in the treatment of various organic pollutants. In order to enhance the photocatalytic degradation,  $\text{TiO}_2$  has been doped with transition metal ions such as V, Fe, Mo, Pd, and Nb to reduce the optical energy gap [16]. In particular, vanadium-doped  $\text{TiO}_2$  can significantly reduce the energy gap from 3.0–3.2 eV to 2.5–2.7 eV [17,18]. The decrease in the bandgap of the vanadium doped  $\text{TiO}_2$  results in visible range excitation and hydroxyl radical generation with low energy. Such vanadium-doped catalysts are usually applied for photocatalytic degradation and the adsorption of pollutants [19,20]. Compared to the photocatalysis, the electrocatalyst can also produce  $\bullet\text{OH}$  with high oxidation capacity. As such, the vanadium-doped  $\text{TiO}_2$  catalyst used in the electrocatalytic technique has potential not only to produce  $\bullet\text{OH}$  under a lower electric field, but to also enhance the electrochemical reaction of pollutants. To further obtain high effectiveness of application, the high specific surface area of the catalyst (i.e., nano size particle) is a useful approach. Accordingly, the vanadium-doped  $\text{TiO}_2$  nanocatalyst used for electrocatalytic treatment is an innovative approach compared to the currently well-known electrocatalysts.

AR 27 is carcinogenic and classified as an endocrine-disrupting substance [21], which is widely used in food, cosmetic, and pharmaceutical products. It typically causes some adverse effects on the natural environment [22], moreover, its inadvertent ingestion induces various health problems. AR 27 is an anionic monoazo dye that has good solubility in water and is not easily handled by traditional physical and chemical wastewater processes [23]. In this work, the nano-vanadium-doped  $\text{TiO}_2$  (nano V/ $\text{TiO}_2$ ) electrode was manufactured by a sol-gel dip-coating method. The effects of manufacturing parameters on catalyst properties including the microstructure, crystal structure, and specific surface area, etc. were investigated respectively. The degradation efficiency of AR 27 dye in an electrocatalytic system by nano V/ $\text{TiO}_2$  electrodes was evaluated to find the optimal operational parameters.

## 2. Results and Discussion

### 2.1. Surface Characteristics of Nano Vanadium-Doped $\text{TiO}_2$ (V/ $\text{TiO}_2$ ) Electrode

Figure 1 shows the field emission scanning electron microscope (FESEM) images of different electrodes. From Figure 1a, it was observed that the  $\text{TiO}_2$  particles could effectively be coated on the titanium substrate by this experimental method. The catalyst mainly exists in the form of round shape particles and has an average size of about 30 nm. Although these particles were arranged in an orderly manner, it had a few impurities on the surface of the catalyst. Figure 1b shows that the particle size of the 0.05 VT catalyst was slightly larger than  $\text{TiO}_2$  due to the doping of vanadium metal, and the average particle size was about 50–80 nm. Meanwhile, the surface of the catalyst was uneven and some particles accumulated into clumps. Figure 1c shows that the particle arrangement of 0.10 VT is regular and catalysts surface also gradually even; with the average particle size of about 50–100 nm.

The particle size of the 0.30 VT catalyst was changed insignificantly and the particle accumulation also became dense (Figure 1d). The real difference is that many long column structures had been produced on the 0.30 VT surface. A similar result was also found by Li et al., whose results showed that the catalysts appeared rod-like shape under the doping of different vanadium weight percentages [24]. From the microstructure observed, the particle accumulation increased with the molar ratio of V to Ti, and the catalyst surface became even. Furthermore, many similar columnar structures appeared on the catalyst surface when the vanadium doped was increased to 0.30 VT. To understand the difference of the vanadium–titanium molar ratios of the prepared catalysts between the theoretical and real, the element ratio of vanadium to titanium atoms in different catalysts was analyzed by energy-dispersive x-ray spectroscopy. It was found that the atomic percentage of titanium in the 0.05 VT, 0.10 VT, and 0.30 VT catalysts were 35.43%, 33.88%, and 28.39%, whereas that of vanadium was 1.45%, 3.40%, and 7.71%, respectively. After conversion, the actual V/Ti ratios were 0.041, 0.10, and 0.27, which was very close to the prepared catalysts in this study.

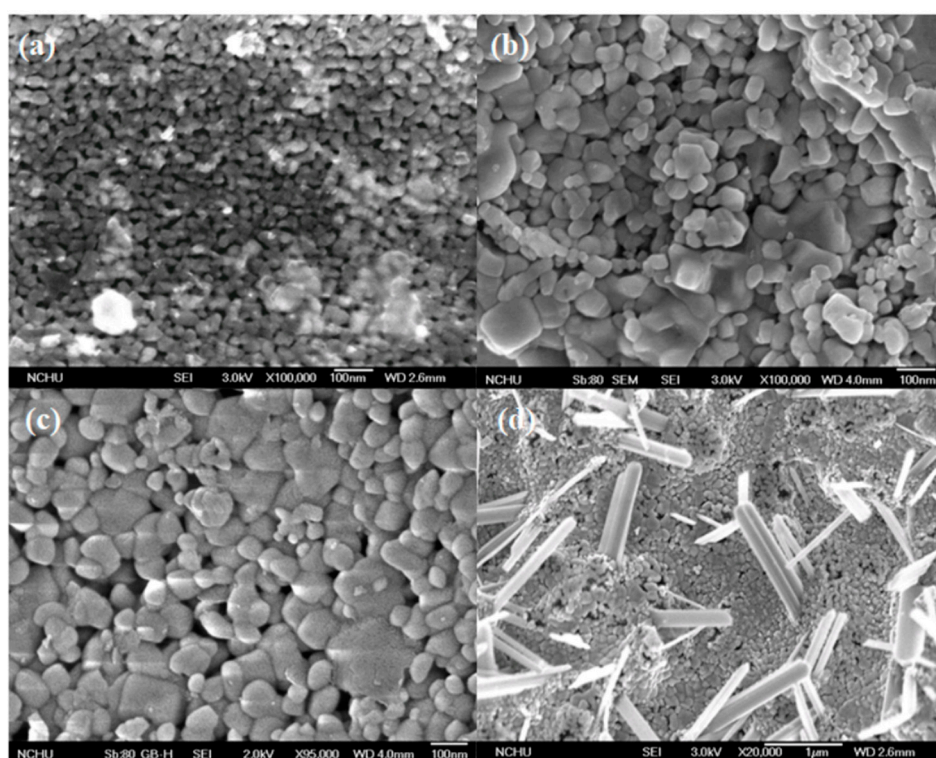


**Figure 1.** Field emission scanning electron microscope (FESEM) images of different electrodes. (a)  $\text{TiO}_2$  (b) 0.05 VT (c) 0.10 VT (d) 0.30 VT.

The crystal structure of the different electrodes identified by the x-ray diffraction analyzer and the resultant peaks were well-matched with the JCPDS (Joint Committee on Powder Diffraction Standards) database. Figure 2 shows the XRD pattern of the 0.1 VT electrode. Along with the Ti peak generated from the substrate, diffraction peaks observed at  $25.3^\circ$ ,  $37^\circ$ ,  $37.8^\circ$ ,  $48^\circ$ ,  $53.8^\circ$ ,  $55^\circ$ , and  $75^\circ$  belonged to the anatase of titanium dioxide [25,26]. Compared to the pure  $\text{TiO}_2$  electrode, the ratio of the anatase crystal was insignificantly decreased (89.6% of pure  $\text{TiO}_2$  and 86% of 0.10 VT), however, the crystal ratio significantly changed when the molar ratio of V to Ti was increased to 0.30. Although the anatase crystal still dominated (about 56.6%), the peak of rutile found at  $27.4^\circ$ ,  $36.1^\circ$ , and  $54.3^\circ$  of  $2\theta$  [27], and the peaks of  $\text{V}_2\text{O}_5$  crystals were also produced (data not shown).

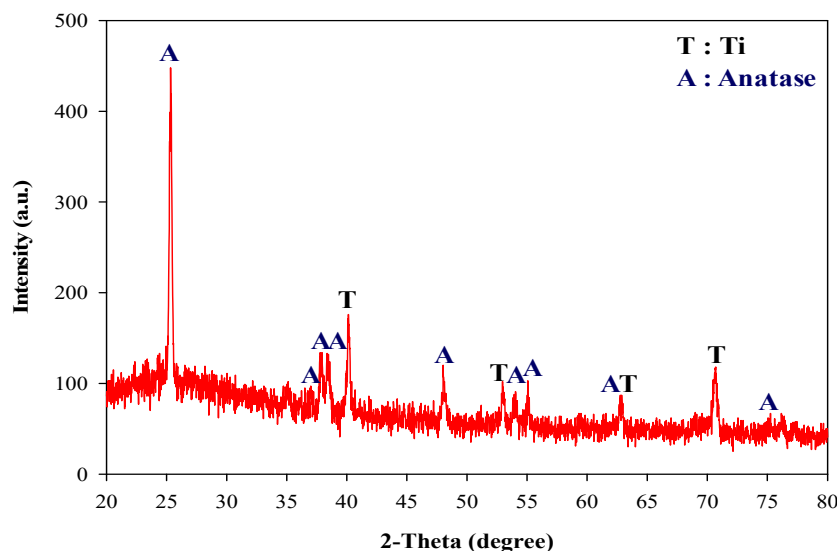


**Figure 2.** X-ray diffraction (XRD) pattern of the 0.10 VT electrode.

The specific surface areas of all electrodes in this study are shown in Table 1. The vanadium-metal increased the specific surface area of the electrode, especially in a 0.10 molar ratio of V to T. The result shows that the specific surface area of the pure  $\text{TiO}_2$  electrode was about  $38 \text{ m}^2 \text{ g}^{-1}$  and the highest was obtained with the 0.10 VT electrode, which was about  $96 \text{ m}^2 \text{ g}^{-1}$ . The high specific surface area of 0.10 VT was attributed to the evenly arranged particles and an increase in the number of catalyst particles. Although 0.30 VT was similar in particle size to 0.10 VT, many columnar structures were produced on the surface, which resulted in a decrease in the specific surface area from 96 to  $79 \text{ m}^2 \text{ g}^{-1}$ . Shee et al. observed that the changes took place in the specific surface area when 2–10 wt%  $\text{V}_2\text{O}_5$  was added to the composite oxide of  $\text{TiO}_2\text{-Al}_2\text{O}_3$ . The specific surface area of 2 wt%  $\text{V}_2\text{O}_5$  was  $91 \text{ m}^2 \text{ g}^{-1}$  and it was significantly decreased to  $73 \text{ m}^2 \text{ g}^{-1}$  at 10 wt% of  $\text{V}_2\text{O}_5$ . The result suggests that the addition of  $\text{V}_2\text{O}_5$  of more than a certain amount resulted in a reduction of the specific surface area [28]. Hence, the appropriate doping of vanadium ions can increase the specific surface area of the catalyst, with more reactive sites to degrade the dye.

**Table 1.** The specific surface area of all electrodes.

Electrode	Specific Surface Area ( $S_{\text{BET}}$ ) ( $\text{m}^2 \text{ g}^{-1}$ )
Pure $\text{TiO}_2$	38
Nano V/ $\text{TiO}_2$ (0.05 VT)	51
Nano V/ $\text{TiO}_2$ (0.10 VT)	96
Nano V/ $\text{TiO}_2$ (0.30 VT)	79

## 2.2. Variation of the Color and Total Organic Carbon (TOC) under Different Electrodes

This study investigated the color degradation and the TOC mineralization of AR 27 dye by the electrocatalytic system. To clarify the effect of the laboratory fluorescent light in the degradation process, the dye was tested by stirring under the fluorescent light of wavelengths 435 nm, 545 nm, and 611 nm with the light intensity less than  $1 \text{ mW cm}^{-2}$ . The whole experiment was performed without a catalytic electrode and controlled at different pH values (3, 6, and 9). The results showed that the dye color and TOC were almost unchanged and the removal efficiencies were lower than 2.2% and 1%, respectively. This indicates that the effect of fluorescent light could be ignored in the degradation of AR 27 dye.

Furthermore, the adsorption efficiency of AR 27 dye in different catalytic electrodes was carried out. The results showed that the adsorption efficiency of the pure  $\text{TiO}_2$  electrode at pH 3 was slightly higher than that of the vanadium-doped electrode. The color removal efficiency of the pure  $\text{TiO}_2$  electrode

was about 8%, while the other electrodes were lower than 2% at 120 min of reaction time. In general, the  $\text{pH}_{\text{zpc}}$  value of the  $\text{TiO}_2$  catalyst is about 5.8. As the pH value of the solution is lower than the  $\text{pH}_{\text{zpc}}$  of  $\text{TiO}_2$ , the catalyst surface will carry a positive charge (Equations (1) and (2)) [27]. The status makes it easier for the anionic dye molecules to become adsorbed on the surface of the pure  $\text{TiO}_2$  catalyst. In contrast, the vanadium-doped catalytic electrodes (0.05 VT, 0.10 VT, and 0.30 VT) adsorption effect was insignificant, and the removal efficiencies were less than 2%. Therefore, the influence of the adsorption reaction in the degradation of the AR 27 dye can be excluded.

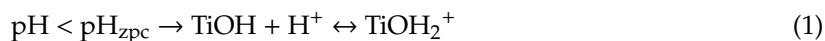
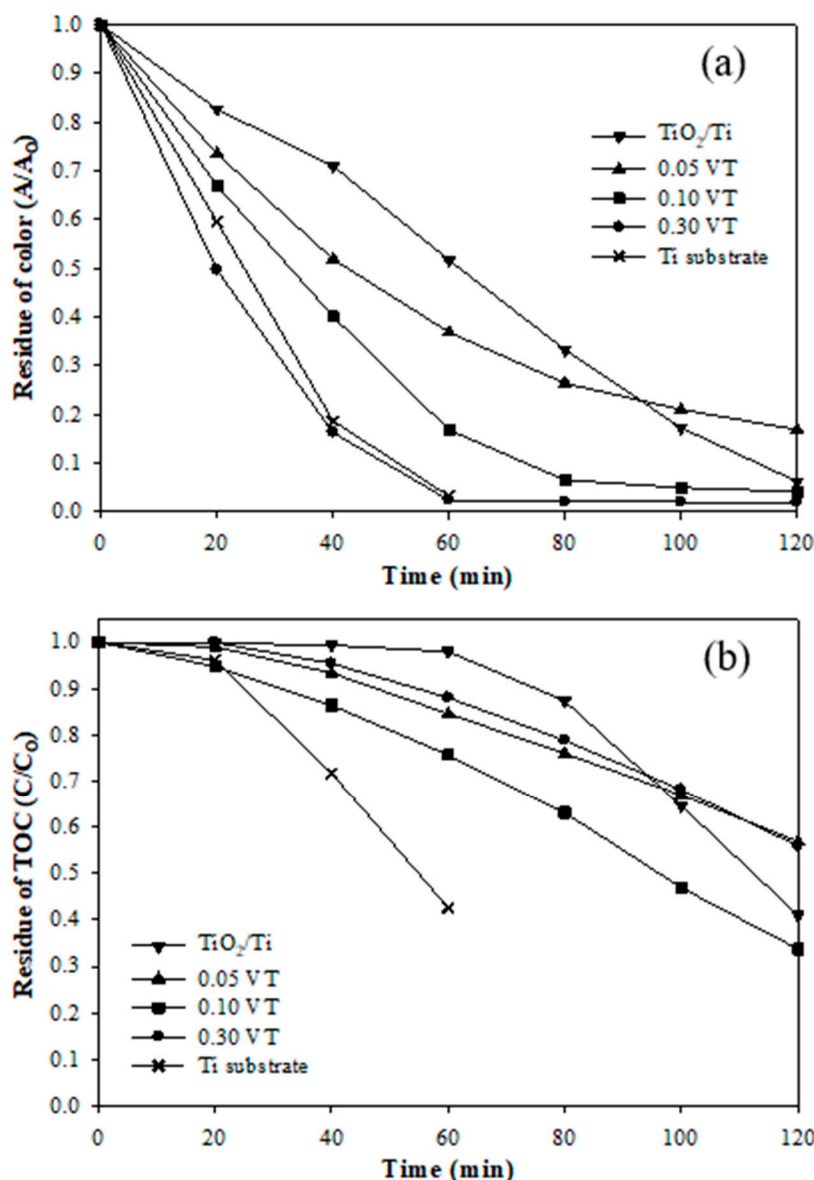


Figure 3 shows the residue of color and TOC at the different catalytic electrodes with operating time. The color removal efficiencies of the  $\text{TiO}_2$ , 0.05 VT, 0.10 VT, and 0.30 VT electrodes were 94%, 83%, 96%, and 98%, respectively. This result indicated that dye color can effectively be removed by the electrocatalytic process. It can be observed that in the 60 min degradation reaction, the removal efficiency of the vanadium-doped catalyst was significantly better than that of the  $\text{TiO}_2$  electrode, with the removal efficiency of 97%, 83%, 63%, and 48%, respectively (0.30 VT > 0.10 VT > 0.05 VT >  $\text{TiO}_2$ ). This phenomenon is most evident that the removal efficiency increased with the vanadium concentration and indicates that the vanadium metal doping to  $\text{TiO}_2$  can effectively increase the color removal. Figure 3b shows the TOC residue of the AR 27 dye in different catalytic electrodes. The TOC removal efficiencies of 0.10 VT,  $\text{TiO}_2$ , 0.30 VT, and 0.05 VT were 66%, 59%, 44%, and 43%, respectively in the treatment time of 120 min. The 0.10 VT had the best TOC mineralization, which was due to the significant effect of the particle arrangement, crystal composition, and the specific surface area.

From the surface structure of the 0.10 VT electrode, the catalyst particles were arranged neatly and uniformly, with no apparent hole produced, which may have a better electron transfer rate for degrading the AR 27 dye. Additionally, the high specific surface area of the catalyst possessed more active sites, which enhanced the contact area between the pollutants and catalyst surface, and hence the degradation efficiency was increased. The 0.10 VT catalytic electrode had the highest specific surface area ( $96 \text{ m}^2 \text{ g}^{-1}$ ), which is consistent with the degradation efficiency of the AR 27 dye.

It was observed that the Ti substrate in the color removal and TOC mineralization had specific effects. The removal efficiencies of color and TOC by the Ti substrate were 96.7% and 57.5%, respectively, at an operating time of 60 min. The removal efficiency of the Ti substrate was much higher than that of the other electrodes at the same operation time. Considering the voltage trend of the system, the voltage variation of the Ti substrate rose to 146 V for 20 min operation and the voltage reached 160 V at 60 min operation. At the same time, the temperature was raised to about  $90^\circ\text{C}$ . Such conditions are not suitable in practical application. In addition, the TOC removal efficiency of the pure  $\text{TiO}_2$  electrode could reach 59% at 120 min of operation time, and the voltage rose significantly after 60 min of operation. These results indicate that the TOC removal has a substantial correlation with the reaction voltage. In contrast, the catalytic electrode after vanadium doped not only had a positive effect on the degradation of pollutants, but also required a relatively small reaction voltage in this electrocatalytic system operation. We speculate that the voltage drop was due to the addition of transition metal to the titanium dioxide, which increased additional charge carriers and effectively reduced the electrical resistance of the material, thereby changing the electronic structure of the original titanium dioxide [29].





**Figure 3.** The residue of (a) the AR 27 dye color and (b) TOC of different catalytic electrodes at a current density of  $20 \text{ mA cm}^{-2}$  during 120 min treatment time.

According to the x-ray photoelectron spectroscopy (XPS) analysis, the catalyst electrodes doped with vanadium metal at different ratios in this study showed the existence of two bands in the V 2p single-element energy spectrum, which were 513.2~518.9 eV (V 2p<sub>3/2</sub>) and 520.4~525.5 eV (V 2p<sub>1/2</sub>). For Supplementary Figure S1, the V 2p<sub>3/2</sub> diffraction peak of 0.05 VT was 516.2 eV, for 0.10 VT it was 516.6 eV, and 0.30 VT was 517 eV. In addition, the V 2p<sub>1/2</sub> diffraction peak of 0.05 VT was 523.6 eV, for 0.10 VT it was 523.8 eV, and the 0.30 VT was 524.4 eV. Since the diffraction peak of V 2p<sub>3/2</sub> was between 516.6 eV and 517.3 eV, it indicates that both V<sup>4+</sup> and V<sup>5+</sup> exist [30]. In addition, when the diffraction peak of V 2p<sub>3/2</sub> was between 516.8 eV and 516.9 eV or 516.4 eV and 517.4 eV, V<sup>5+</sup> was present, and between 515.4 eV and 515.7 eV or 516.3 eV was V<sup>4+</sup> [31,32]; for the V 2p<sub>1/2</sub> diffraction peak at 523.6 eV, it was V<sup>4+</sup> and at 524.5 eV it was V<sup>5+</sup> [33]. The results confirmed that V had been doped on the surface of the catalyst, which mainly existed in the form of V<sup>4+</sup> and V<sup>5+</sup> bonds. At the nano V/TiO<sub>2</sub> catalyst anode, the V<sup>4+</sup> was oxidized to form V<sup>5+</sup> (Equation (3)). Then, the V<sup>5+</sup> reacted with the hydroxide ion to form hydroxide radicals (Equation (4)) [34], or the hydroxide ions carried out electrochemical oxidation (Equation (5)), which promoted the degradation of the AR 27 dye. Considering the pH trend of the wastewater, the vanadium doped catalyst electrode increased the

initial value of 5.9 to a maximum of 7.1 (data not shown) while the pure titanium dioxide was increased to 10. The vanadium doped electrode changed the pH value to a small extent, which met the results of Equations (4) and (5).



As far as the conductivity of the wastewater was concerned, the titanium dioxide electrode increased from  $4650 \mu\text{S cm}^{-1}$  to  $4930 \mu\text{S cm}^{-1}$ . The remaining doped catalyst electrodes increased the value to the highest of  $4821 \mu\text{S cm}^{-1}$ . The results show that the variation of conductivity remained relatively stable in this electrocatalytic system. The temperature change in water quality is also an important environmental indicator. According to the changing trend, it can be seen that the titanium dioxide electrode increased the temperature from  $23^\circ\text{C}$  to  $80^\circ\text{C}$ , and the other vanadium-doped catalyst electrodes to  $60^\circ\text{C}$ , indicating that vanadium-doped electrodes can reduce the temperature of the system. The electrocatalytic technique is suitable for advanced wastewater treatment after biological treatment, where the color remains sustained in the pollutants, even when the organic matter has been decomposed. The current electrocatalytic technique can quickly decolorize the dye. According to the results of this study, the color can be effectively removed under the vanadium-doped electrode at 1 h of operation time. At this time, the increase in temperature remains relatively gentle (increased about  $38^\circ\text{C}$ ). Therefore, the vanadium-doped electrode can achieve color removal with less energy consumption.

In the current electrocatalytic system, dye decolorization occurs through anodic oxidation [35], partial cathodic reduction [36], and some other complex procedures. The research on the degradation and decolorization of pollutants caused by oxidation or reduction will be discussed in subsequent studies. AR 27 dye is mainly composed of the azo bond ( $\text{N}=\text{N}$ ), naphthalene ring, and sulfonic groups ( $\text{SO}_3\text{H}$ ), in which the azo bond has the most active site in the degradation reaction. The first step of degradation of the AR 27 dye takes place by an oxidant ( $\bullet\text{OH}$ ) carrying out  $\text{N}-\text{N}$  bond cleavage, which leads to quick decolorization of the dye. Then, the amine's aromatic compound is produced [37], followed by further oxidation. After the successful cleavage of the azo bond, the sulfuric acid group in the amines is removed and the two isomers are generated. After a series of oxidation reactions by the oxidants, the isomers are converted into phthalic anhydride and subsequently transferred into benzoic acid derivate and phenol products. In the next step, the oxidation of the aromatic ring through  $\bullet\text{OH}$  takes place to form the phenol hydroxyl derivatives, which are subsequently converted into aliphatic acid intermediates by the breakdown of the aromatic ring structure. The intermediate products include m-hydroxy-benzoic acid, malonic, and oxalic acid, and the final mineralized to  $\text{CO}_2$  and  $\text{H}_2\text{O}$ . A detailed degradation pathway of AR 27 has been published by Steter et al. [35]. This experimental result shows that the nano  $\text{V}/\text{TiO}_2$  electrode can effectively mineralize AR 27 with a high removal efficiency of TOC.

### 2.3. Variation of the Color and TOC under a Different Current Density

Figure 4 shows the color and TOC residues of the 0.10 VT catalytic electrode at different current density. Figure 4a indicates that the color was stably removed under the current density of  $10 \text{ mA cm}^{-2}$ , for which the removal efficiency was about 97%. When the current density was controlled at 15 and  $20 \text{ mA cm}^{-2}$ , the removal efficiency reached 96% and 98%, respectively. As the current density was increased to  $25 \text{ mA cm}^{-2}$ , the color removal efficiency rapidly reached 98% at 40 min treatment, which showed a significant reduction in the operating time. The degradation of dye was attributed to the generation of a high concentration of hydroxyl radicals under a high current density, which destroys the chromogen to achieve fast color removal [4]. Figure S2 shows the color change of the AR 27 dye with a current density of  $25 \text{ mA cm}^{-2}$ . It was observed that the original color of AR 27 was purple-red and the water sample became almost transparent and colorless after 40 min of

treatment, indicating that the 0.10 VT electrode can rapidly and effectively remove the AR 27 dye in the wastewater. Figure 4b shows the TOC residue of the 0.10 VT electrode at different current densities. It was found that the removal efficiencies of TOC were 31% and 38% when the electrocatalytic system was provided with a relatively low current density (10 and 15 mA cm<sup>-2</sup>). The degradation mechanism of pollutants by the electrocatalyst is divided into direct oxidation of the electrode and the indirect oxidation of organic matter by hydroxyl radicals [38]. As the current density is lower, not only is the ability of direct oxidation limited, but also the generation of hydroxyl radicals.

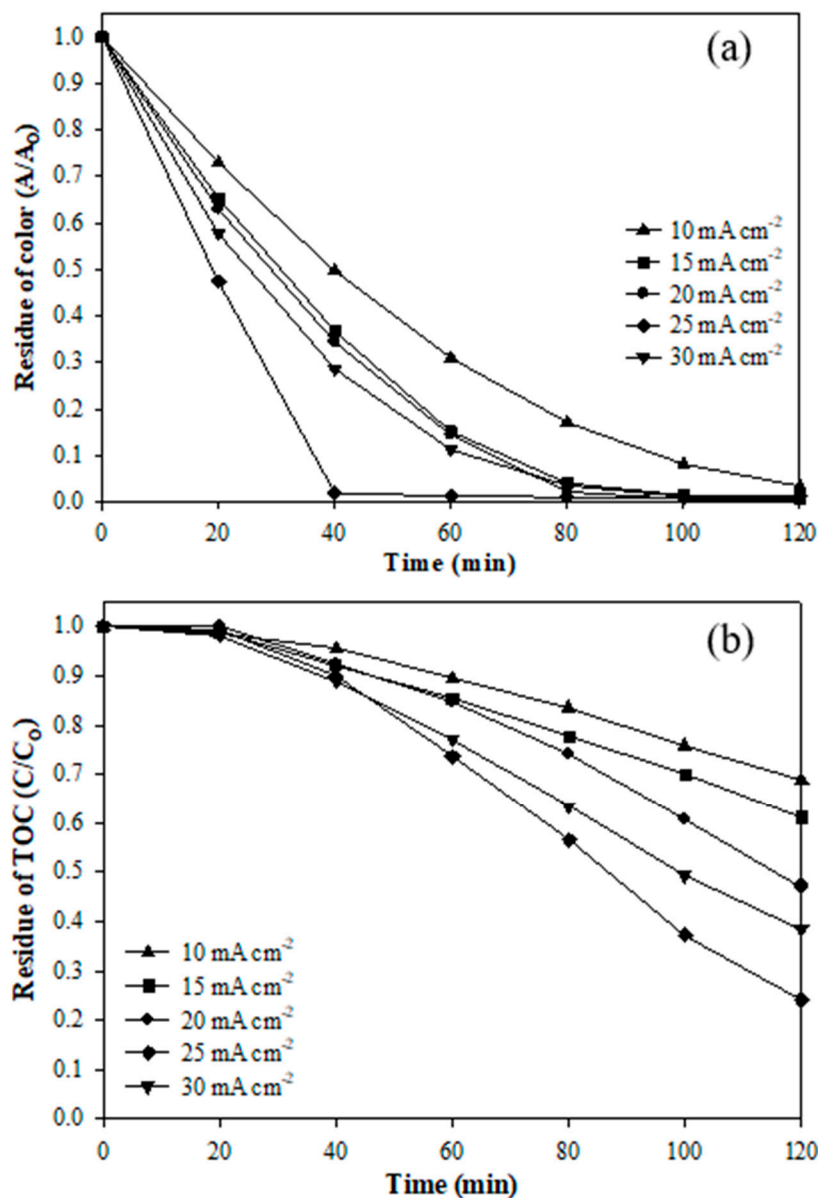


**Figure 4.** The residue of (a) the AR 27 dye color and (b) TOC of 0.10 VT at current densities (10–30 mA cm<sup>-2</sup>) during 120 min treatment time.

The removal efficiency of TOC in the dye was significantly improved under the current density of 25 mA cm<sup>-2</sup>, where the highest was reached at around 76%. Theoretically, the electron transfer rate of pollutants increased with the current density, resulting in higher removal efficiency [38]. However, the hydrolysis reaction was intense when the current density increased to 30 mA cm<sup>-2</sup> and the by-product oxygen was also produced rapidly due to the high current density [39,40]. Oxygen will take part in a competitive reaction with the pollutants, resulting in a decrease in hydroxyl radicals



to degrade the TOC. Therefore, the  $25 \text{ mA cm}^{-2}$  current density is the most suitable operation for this experiment. Additionally, this study evaluated the kinetic mode for degrading the AR 27 dye. The TOC mineralization was more consistent with the zero-order reaction kinetic, and the 0.10 VT had the maximum reaction rate constant ( $k = 1.06 \times 10^{-6} \text{ M min}^{-1}$ ). Furthermore, the color removal with different catalytic electrodes was more consistent with the first-order reaction kinetic.

To understand the cost of electrocatalytic degradation, the energy consumption of different electrodes was calculated. The electrical consumption of dye decolorization was evaluated by the overall electrocatalytic reaction as well as the oxidation, reduction, and other electrochemical reactions. Since the color removal efficiency of the 0.05 VT catalytic electrode was about 80% at 120 min of treatment, it was used as a calculation standard. Table 2 shows the electrical consumption of different catalytic electrodes. The electrical consumptions of pure  $\text{TiO}_2$ , 0.05 VT, 0.10 VT, and 0.30 VT were 0.11, 0.08, 0.04, and 0.02  $\text{kWh L}^{-1}$ , respectively. Considering the reaction voltage of  $\text{TiO}_2$  was much higher than that of the vanadium-doped catalytic electrodes and the operation time was longer, the energy consumption was 2.75 and 5.5 times for the 0.10 VT and 0.30 VT, respectively. A small amount of  $\text{V}_2\text{O}_5$  (vanadium oxide) was produced after doping the vanadium metal to  $\text{TiO}_2$  in this study. Based on the electrical conductivity of the material, the  $\text{TiO}_2$  and  $\text{V}_2\text{O}_5$  were noted to be  $10^{-5}\sim 10^{-8} \text{ S m}^{-1}$  and  $10^{-3}\sim 10^{-5} \text{ S m}^{-1}$ , respectively [41]. This confirms that the change in the conductivity of the electrocatalytic system takes place with the formation of vanadium oxide. Moreover, in the analysis of the electrochemical with voltage–current response curve in this study, the maximum current density of  $\text{TiO}_2$  was 7.27 mA and 0.30 VT was 12.2 mA under the fixed voltage of 3.0 V (data not shown), which shows that the vanadium doped electrode has a relatively high response current. Therefore, the vanadium doped electrode can save the cost of electricity consumption in this electrocatalytic system.

**Table 2.** The electricity consumption of all electrodes for the decolorization of AR 27.

Item	Pure $\text{TiO}_2$	0.05 VT	0.10 VT	0.30 VT
Average voltage (V)	74	46	48	39
Treatment time (min)	100	120	60	40
Electrical consumption ( $\text{kWh L}^{-1}$ )	0.11	0.08	0.04	0.02

Karkmaz et al. used the Degussa P-25 titanium dioxide powder to degrade AR 27 (TOC of  $17 \text{ mg L}^{-1}$ ), and irradiated it with a 125 W high-pressure mercury lamp with a photon flux of  $6 \times 10^{-6} \text{ mol photons s}^{-1}$ . The report showed that the color of the dye could be completely removed under UV light for 2.5 h and the removal efficiencies of COD and TOC were 65% and 30%, respectively [42]. In the electrochemical degradation, the  $100 \text{ mg L}^{-1}$  of AR 27 dye was tested on the boron-doped diamond electrode (BDD) at a current density of  $35 \text{ mA cm}^{-2}$ . The data indicated that a TOC removal efficiency of 92% could be obtained after 90 min of operation [35]. According to their results, the electrocatalytic system possessed higher treatment efficiency than the photocatalyst due to the advantage of treatment time and TOC mineralization. Additionally, the cost of the vanadium doped  $\text{TiO}_2$  catalytic electrode is relatively low when compared with the BDD electrode, which increases the potential of practical application.

To consider the electrode's long-term use, the 0.10 VT electrode was tested to observe the removal efficiency of the dye color during reuse. Figure 5 shows the residue of the color for the 0.10 VT electrode with different operation times. The result shows that the color removal efficiency could reach about 99% under the electrode repeated usage. Meanwhile, the catalysts were not peeled off significantly under repeated use; the weight loss of the catalyst was only about 3% and 5% under one time and three times of usage, respectively. The results indicate that the nano V/ $\text{TiO}_2$  electrode did not only effectively degrade the AR 27 dye, but also could be used repeatedly.

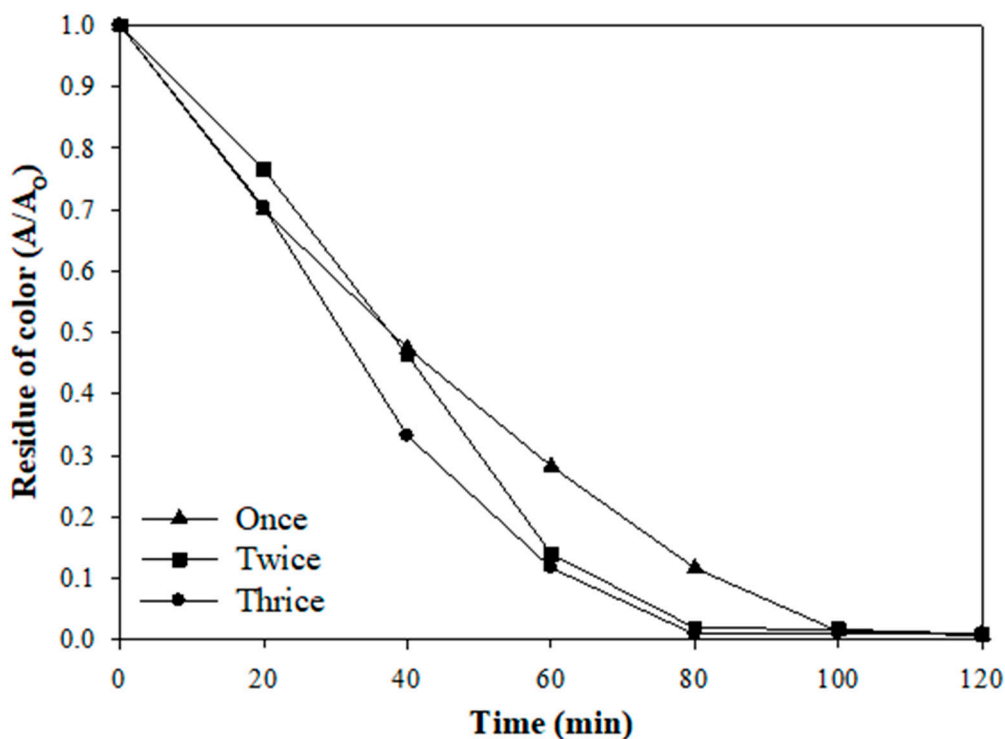


Figure 5. The repeatability test of the 0.10 VT electrode for degrading the AR 27 dye.

### 3. Experimental

#### 3.1. Preparation of Nano V/TiO<sub>2</sub> Electrode

Vanadyl acetylacetonate ( $\text{VO}(\text{C}_5\text{H}_7\text{O}_2)_2$ ; purity of 98%; Aldrich) was the vanadium precursor and other chemicals included titanium (IV) isopropoxide ( $\text{Ti}(\text{OC}_3\text{H}_7)_4$ ; purity > 98%; ACROS, Geel, Belgium), acetic acid ( $\text{CH}_3\text{COOH}$ ; purity > 99.9%; JT Baker, Phillipsburg, NJ, USA), and isopropyl alcohol ( $\text{CH}_3\text{CHOCH}_3$ ; purity of 99.5%; JT Baker, Phillipsburg, NJ, USA). The preparation steps of the V/TiO<sub>2</sub> electrode are shown in Figure S3. In the beginning, a certain amount of vanadium precursor was directly added to the TiO<sub>2</sub> catalyst sol. The molar ratio of vanadium to titanium was 0.05, 0.10, and 0.30, and named as 0.05 VT, 0.10 VT, and 0.30 VT, respectively. Then, the mixed solution was stirred with 600 rpm for 15 h to obtain the fine suspended sol. Subsequently, the prepared sol was poured into a 100 mL graduated cylinder, and the titanium substrate was slowly immersed in the sol. After 60 s of impregnation, the vanadium doped TiO<sub>2</sub> electrode was pulled up at a rate of 45 cm min<sup>−1</sup>, and the volatile solvents and moisture were removed by an oven at 105 °C for 15 min. Finally, the electrode was calcined at 500 °C for 1.5 h in a high-temperature furnace.

The above impregnating, drying, and calcining steps were repeated six times while the sixth time was calcined at 500 °C for 24 h. Finally, the V/TiO<sub>2</sub> electrode was ultrasonicated for 15 min to remove the catalyst with weak surface adhesion. The prepared V/TiO<sub>2</sub> electrode was observed by field emission scanning electron microscope (FESEM, JEOL-JSM-6700F, Tokyo, Japan) and energy-dispersive x-ray spectroscopy (EDS, OXFORD INCA ENERGY 400, Britain) to obtain the surface morphology and chemical composition. A powder x-ray diffractometer (MXP18 diffractometer with Cu K $\alpha$  radiation,  $\lambda = 1.54056 \text{ \AA}$ , MAC Science Co., Ltd, Tokyo, Japan) was used to identify the crystal structure. The specific surface area was measured using a Brunauer–Emmett–Teller (BET) technique (PMI BET 201 AC, Germany).

#### 3.2. Degradation of AR 27 Dye

The AR 27 dye was the target pollutant in this study, in which the chemical structure and other properties are listed in Table S1. In this experiment, sodium sulfate ( $\text{Na}_2\text{SO}_4$ , 98%, Merck, Darmstadt, Germany) was used as the electrolyte and the pH of the wastewater containing dye

was adjusted with 0.01 M nitric acid and sodium hydroxide. Figure S4 shows the electrocatalytic system for treating the AR 27 dye. The glass reactor with a 9 cm diameter and 18 cm in height was used and the wastewater volume was around 1 L. The reactor included a pair of electrodes, and the different molar ratios of V/TiO<sub>2</sub> served as anodes while graphite was used as the cathode for all experiments. The distance between the cathode and anode was 6.0 cm, and all electrodes had the same size (16 cm length × 2.5 cm width × 0.3 cm thickness). DC power supply was used (GW Instek, GPR-20H20D, Taiwan) to provide constant current for the electrocatalytic system. An electromagnetic stirrer (Corning, PC420D, Stirrer/Hot, New York, USA) promoted the uniformity of the AR 27 dye.

Table S2 lists the operating parameters of the electrocatalytic experiment. All degradation experiments were carried out in 22.5 mM Na<sub>2</sub>SO<sub>4</sub> electrolyte for 120 min of operation. The color measurement of the AR 27 dye was conducted by a UV-Visible spectrophotometer (JASCO, V-650, Tokyo, Japan) operating at the maximum absorption wavelength (521 nm). In addition, the TOC variation of AR 27 dye in fixed time intervals was analyzed according to the Taiwan Environmental Protection Agency (EPA) method (NIEA W530.51C). In this study, a 10 mL sample was collected each time and filtered through 0.22 µm filter paper, then analyzed by a total organic carbon analyzer (TOC-VCSN, Shimadzu, Japan). The flow rate of the sample was controlled at 130 mL min<sup>-1</sup> and the gas pressure was 200 KPa. After the automatic suction device drew the sample, 2 N HCl was added to acidify the sample to attain a pH value less than 2, in which the inorganic carbon in the sample becomes CO<sub>2</sub>. Then, the CO<sub>2</sub> was removed by zero-level air to complete the pre-treatment of the sample. Finally, 50 µL of the sample was drawn for analysis.

Apart from the color and TOC analysis, the pH, conductivity, and temperature were also measured under electrocatalytic experiments at every 20 min time interval. Moreover, electrical energy consumption was also studied to estimate the economical competency of the nano V/TiO<sub>2</sub> electrode in treating the AR 27 dye. The formula for energy consumption is as shown in Equation (6) [43] and the calculated result takes per kWh (kilowatt-hour) as the unit.

$$\text{Energy consumption (kWh L}^{-1}\text{)} = \frac{UIT}{V} \quad (6)$$

where U is the average voltage (V); I is the current (A); T is the operation time (h); and V is the reaction volume (L).

#### 4. Conclusions

After discussing and explaining the experimental results, several conclusions can be drawn:

1. The AR 27 dye was effectively degraded by the different molar ratios of nano V/TiO<sub>2</sub> electrodes; the color and total organic carbon (TOC) removal efficiencies of the 0.10 VT electrode reached to 99% and 76%, respectively.
2. The high specific surface area (38 m<sup>2</sup> g<sup>-1</sup> to 96 m<sup>2</sup> g<sup>-1</sup>) of the nano V/TiO<sub>2</sub> electrode facilitated the electrocatalytic degradation.
3. The current density of 25 mA cm<sup>-2</sup> was the optimal operation for this electrocatalytic system; the production of oxygen as a by-product was more pronounced when the current density was increased to 30 mA cm<sup>-2</sup>.
4. The electricity consumption of the pure TiO<sub>2</sub> and nano V/TiO<sub>2</sub> electrode in the electrocatalytic system was 0.11 kWh L<sup>-1</sup> and 0.02 kWh L<sup>-1</sup>, respectively.
5. The results indicate that the nano V/TiO<sub>2</sub> electrode not only effectively degraded the AR 27, but could also be used repeatedly; the dye removal efficiency attained 99% even with repeated usage.

**Supplementary Materials:** The following are available online at <http://www.mdpi.com/2073-4344/10/5/482/s1>, Figure S1: The V 2p single-element energy spectrum in different vanadium metal ratios; Figure S2: The color change of AR 27 dye wastewater with a treatment time of 0–120 min (from left to right); Figure S3: The preparation process of the nano V/TiO<sub>2</sub> electrode during the sol-gel method; Figure S4: The schematic diagram of the electrocatalytic system, Table S1: Properties of the AR 27 dye; Table S2: Experimental conditions of electrocatalytic degradation.

**Author Contributions:** Conceptualization and methodology—J.-H.C., C.-D.D. and S.-Y.S.; formal analysis, investigation and data curation—S.-Y.S.; writing—original draft preparation—S.-Y.S. and Y.-L.W.; writing—review and editing—J.-H.C. and S.-Y.S.; supervision—J.-H.C. and C.-D.D. All authors have read and agreed to the published version of the manuscript.

**Funding:** This research received no external funding.

**Conflicts of Interest:** The authors declare no conflicts of interest.

## References

- Shen, Z.M.; Wu, D.; Yang, J.; Yuan, T.; Wang, W.H.; Jia, J.P. Methods to improve electrochemical treatment effect of dye wastewater. *J. Hazard. Mater.* **2006**, *131*, 90–97. [CrossRef] [PubMed]
- Basiri Parsa, J.; Rezaei, M.; Soleymani, A.R. Electrochemical oxidation of an azo dye in aqueous media investigation of operational parameters and kinetics. *J. Hazard. Mater.* **2009**, *168*, 997–1003. [CrossRef]
- Zhou, M.; He, J. Degradation of azo dye by three clean advanced oxidation processes: Wet oxidation, electrochemical oxidation and wet electrochemical oxidation—A comparative study. *Electrochim. Acta* **2007**, *53*, 1902–1910. [CrossRef]
- Song, S.; Fan, J.; He, Z.; Zhan, L.; Liu, Z.; Chen, J.; Xu, X. Electrochemical degradation of azo dye C.I. Reactive Red 195 by anodic oxidation on Ti/SnO<sub>2</sub>-Sb/PbO<sub>2</sub> electrodes. *Electrochim. Acta* **2010**, *55*, 3606–3613. [CrossRef]
- Cameselle, C.; Pazos, M.; Sanromán, M.A. Selection of an electrolyte to enhance the electrochemical decolourisation of indigo. Optimisation and scale-up. *Chemosphere* **2005**, *60*, 1080–1086. [CrossRef] [PubMed]
- Bouras, H.D.; Isik, Z.; Arıkan, E.B.; Bouras, N.; Chergui, A.; Yatmaz, H.C.; Dizge, N. Photocatalytic oxidation of azo dye solutions by impregnation of ZnO on fungi. *Biochem. Eng. J.* **2019**, *146*, 150–159. [CrossRef]
- Brindha, R.; Muthuselvan, P.; Senthilkumar, S.; Rajaguru, P. Fe<sup>0</sup> catalyzed photo-Fenton process to detoxify the biodegraded products of azo dye Mordant Yellow 10. *Chemosphere* **2018**, *201*, 77–95. [CrossRef]
- Pacheco-Álvarez, M.O.A.; Picos, A.; Pérez-Segura, T.; Peralta-Hernández, J.M. Proposal for highly efficient electrochemical discoloration and degradation of azo dyes with parallel arrangement electrodes. *J. Electroanal. Chem.* **2019**, *838*, 195–203. [CrossRef]
- Li, J.; Zheng, L.; Li, L.; Xian, Y.; Jin, L. Fabrication of TiO<sub>2</sub>/Ti electrode by laser-assisted anodic oxidation and its application on photoelectrocatalytic degradation of methylene blue. *J. Hazard. Mater.* **2007**, *139*, 72–78. [CrossRef]
- Lissens, G.; Pieters, J.; Verhaege, M.; Pinoy, L.; Verstraete, W. Electrochemical degradation of surfactants by intermediates of water discharge at carbon-based electrodes. *Electrochim. Acta* **2003**, *48*, 1655–1663. [CrossRef]
- Panizza, M.; Martinez-Huitle, C.A. Role of electrode materials for the anodic oxidation of a real landfill leachate—comparison between Ti–Ru–Sn ternary oxide, PbO<sub>2</sub> and boron-doped diamond anode. *Chemosphere* **2013**, *90*, 1455–1460. [CrossRef]
- Zhao, G.; Gao, J.; Shi, W.; Liu, M.; Li, D. Electrochemical incineration of high concentration azo dye wastewater on the in situ activated platinum electrode with sustained microwave radiation. *Chemosphere* **2009**, *77*, 188–193. [CrossRef]
- Tung, C.H.; Chang, J.H.; Hsieh, Y.H.; Hsu, J.C.; Ellis, A.V.; Liu, W.C.; Yan, R.H. Comparison of hydroxyl radical yields between photo- and electro-catalyzed water treatments. *J. Taiwan Inst. Chem. Eng.* **2014**, *45*, 1649–1654. [CrossRef]
- Saini, K.K.; Sharma, S.D.; Chanderkant, K.M.; Singh, D.; Sharma, C.P. Structural and optical properties of TiO<sub>2</sub> thin films derived by sol-gel dip coating process. *J. Non-Cryst. Solids* **2007**, *353*, 2469–2473. [CrossRef]
- Wang, H.; Niu, J.; Long, X.; He, Y. Sonophotocatalytic degradation of methyl orange by nano-sized Ag/TiO<sub>2</sub> particles in aqueous solutions. *Ultrason. Sonochem.* **2008**, *15*, 386–392. [CrossRef]

16. Tripathi, A.M.; Nair, R.G.; Samdarshi, S.K. Visible active silver sensitized vanadium titanium mixed metal oxide photocatalyst nanoparticles through sol-gel technique. *Sol. Energy Mater. Sol. C* **2010**, *94*, 2379–2385. [\[CrossRef\]](#)
17. Chang, S.M.; Liu, W.S. Surface doping is more beneficial than bulk doping to the photocatalytic activity of vanadium-doped TiO<sub>2</sub>. *Appl. Catal. B-Environ.* **2011**, *101*, 333–342. [\[CrossRef\]](#)
18. Masih, D.; Yoshitake, H.; Izumi, Y. Photo-oxidation of ethanol on mesoporous vanadium-titanium oxide catalysts and the relation to vanadium (IV) and (V) sites. *Appl. Catal. A-Gen.* **2007**, *325*, 276–282. [\[CrossRef\]](#)
19. Pal, K.; Ghorai, K.; Aggrawal, S.; Mandal, T.K.; Mohanty, P.; Seikh, M.M.; Gayen, A. Remarkable Ti-promotion in vanadium doped anatase titania for methylene blue adsorption in aqueous medium. *J. Environ. Chem. Eng.* **2018**, *6*, 5212–5220. [\[CrossRef\]](#)
20. Rossi, G.; Pasquini, L.; Catone, D.; Piccioni, A.; Patelli, N.; Paladini, A.; Molinari, A.; Caramori, S.; O’Keeffe, P.; Boscherini, F. Charge carrier dynamics and visible light photocatalysis in vanadium-doped TiO<sub>2</sub> nanoparticles. *Appl. Catal. B-Environ.* **2018**, *237*, 603–612. [\[CrossRef\]](#)
21. Pérez-Urquiza, M.; Beltrán, J.L. Determination of dyes in foodstuffs by capillary zone electrophoresis. *J. Chromatogr. A* **2000**, *898*, 271–275. [\[CrossRef\]](#)
22. Yadav, P.; Meena, R.C. Photo catalytic bleaching of Amaranth by Methylene Blue immobilized resin Dowex-11. *Der Pharm. Lett.* **2010**, *2*, 66–71.
23. Salazar-Gastélum, M.I.; Reynoso-Soto, E.A.; Lin, S.W.; Perez-Sicairos, S.; Félix-Navarro, R.M. Electrochemical and Photoelectrochemical Decoloration of Amaranth Dye Azo Using Compositing Dimensional Stable Anodes. *J. Environ. Prot.* **2013**, *4*, 136–143. [\[CrossRef\]](#)
24. Li, L.; Liu, C.Y.; Liu, Y. Study on activities of vanadium (IV/V) doped TiO<sub>2</sub>(R) nanorods induced by UV and visible light. *Mater. Chem. Phys.* **2009**, *113*, 551–557. [\[CrossRef\]](#)
25. Doong, R.A.; Chang, P.Y.; Huang, C.H. Microstructural and photocatalytic properties of sol-gel-derived vanadium-doped mesoporous titanium dioxide nanoparticles. *J. Non-Cryst. Solids* **2009**, *355*, 2302–2308. [\[CrossRef\]](#)
26. Li, H.; Zhao, G.; Chen, Z.; Han, G.; Song, B. Low temperature synthesis of visible light-driven vanadium doped titania photocatalyst. *J. Colloid Interface Sci.* **2010**, *344*, 247–250. [\[CrossRef\]](#)
27. Ahmed, S.; Rasul, M.G.; Martens, W.N.; Brown, R.; Hashib, M.A. Advances in heterogeneous photocatalytic degradation of phenols and dyes in wastewater: A review. *Water Air Soil Pollut.* **2011**, *215*, 3–29. [\[CrossRef\]](#)
28. Shee, D.; Deo, G.; Hirt, A.M. Characterization and reactivity of sol-gel synthesized TiO<sub>2</sub>-Al<sub>2</sub>O<sub>3</sub> supported vanadium oxide catalysts. *J. Catal.* **2010**, *273*, 221–228. [\[CrossRef\]](#)
29. Yang, S.Y.; Choo, Y.S.; Kim, S.; Lim, S.K.; Lee, J.; Park, H. Boosting the electrocatalytic activities of SnO<sub>2</sub> electrodes for remediation of aqueous pollutants by doping with various metals. *Appl. Catal. B-Environ.* **2012**, *111–112*, 317–325. [\[CrossRef\]](#)
30. Gu, D.E.; Yang, B.C.; Hu, Y.D. A novel method for preparing V-doped titanium dioxide thin film photocatalysts with high photocatalytic activity under visible light irradiation. *Catal. Lett.* **2007**, *118*, 254–259. [\[CrossRef\]](#)
31. Yang, X.; Cao, C.; Hohn, K.; Erickson, L.; Maghirang, R.; Hamal, D.; Klabunde, K. Highly visible-light active C- and V-doped TiO<sub>2</sub> for degradation of acetaldehyde. *J. Catal.* **2007**, *252*, 296–302. [\[CrossRef\]](#)
32. Reddy, B.M.; Sreekanth, P.M.; Reddy, E.P. Surface characterization of La<sub>2</sub>O<sub>3</sub>-TiO<sub>2</sub> and V<sub>2</sub>O<sub>5</sub>/La<sub>2</sub>O<sub>3</sub>-TiO<sub>2</sub> catalysts. *J. Phys. Chem. B* **2002**, *106*, 5695–5700. [\[CrossRef\]](#)
33. Xu, C.; Ma, L.; Liu, X.; Qiu, W.; Su, Z. A novel reduction-hydrolysis method of preparing VO<sub>2</sub> nanopowders. *Mater. Res. Bull.* **2004**, *39*, 881–886. [\[CrossRef\]](#)
34. Tian, B.; Li, C.; Gu, F.; Jiang, H.; Hu, Y.; Zhang, J. Flame sprayed V-doped TiO<sub>2</sub> nanoparticles with enhanced photocatalytic activity under visible light irradiation. *Chem. Eng. J.* **2009**, *151*, 220–227. [\[CrossRef\]](#)
35. Steter, J.R.; Barros, W.R.P.; Lanza, M.R.V.; Motheo, A.J. Electrochemical and sonoelectrochemical processes applied to amaranth dye degradation. *Chemosphere* **2014**, *117*, 200–207. [\[CrossRef\]](#)
36. Jain, R.; Sharma, N.; Radhapyari, K. Electrochemical treatment of pharmaceutical azo dye amaranth from waste water. *J. Appl. Electrochem.* **2009**, *39*, 577–582. [\[CrossRef\]](#)
37. Zhang, G.; Yang, F.; Liu, L. Comparative study of Fe<sup>2+</sup>/H<sub>2</sub>O<sub>2</sub> and Fe<sup>3+</sup>/H<sub>2</sub>O<sub>2</sub> electro-oxidation systems in the degradation of amaranth using anthraquinone/polypyrrole composite film modified graphite cathode. *J. Electroanal. Chem.* **2009**, *632*, 154–161. [\[CrossRef\]](#)



38. Chang, J.H.; Ellis, A.V.; Hsieh, Y.H.; Tung, C.H.; Shen, S.Y. Electrocatalytic characterization and dye degradation of Nano-TiO<sub>2</sub> electrode films fabricated by CVD. *Sci. Total Environ.* **2009**, *407*, 5914–5920. [[CrossRef](#)]
39. Bensalah, N.; Akfaro, M.S.Q.; Martínez-Huitle, C.A. Electrochemical treatment of synthetic wastewater containing Alphazurine A dye. *Chem. Eng. J.* **2009**, *149*, 348–352. [[CrossRef](#)]
40. Panizza, M.; Barbucci, A.; Ricotti, R.; Cerisola, G. Electrochemical degradation of methylene blue. *Sep. Purif. Technol.* **2007**, *54*, 382–387. [[CrossRef](#)]
41. Margha, F.H.; El-Bassyouni, G.T.; Turkey, G.M. Enhancing the electrical conductivity of vanadate glass system (Fe<sub>2</sub>O<sub>3</sub>, B<sub>2</sub>O<sub>3</sub>, V<sub>2</sub>O<sub>5</sub>) via doping with sodium or strontium cations. *Ceram. Int.* **2019**, *451*, 1838–11843. [[CrossRef](#)]
42. Karkmaz, M.; Puzenat, E.; Guillard, C.; Herrmann, J.M. Photocatalytic degradation of the alimentary azo dye amaranth Mineralization of the azo group to nitrogen. *Appl. Catal. B* **2004**, *51*, 183–194. [[CrossRef](#)]
43. Costa, C.R.; Olivi, P. Effect of chloride concentration on the electrochemical treatment of a synthetic tannery wastewater. *Electrochim. Acta* **2009**, *54*, 2046–2052. [[CrossRef](#)]



© 2020 by the authors. Licensee MDPI, Basel, Switzerland. This article is an open access article distributed under the terms and conditions of the Creative Commons Attribution (CC BY) license (<http://creativecommons.org/licenses/by/4.0/>).